Mechanism and Kinetics of the Catalytic CO−H_2 Reaction: An Approach by Chemical Transients and Surface Relaxation Spectroscopy†

Alfred Frennet, Thierry Visart de Bocarmé, Jean-Marie Bastin, and Norbert Kruse*

Chimie Physique des Matériaux (Catalyse-Tribologie), Université Libre de Bruxelles, Campus Plaine, CP 243, 1050 Bruxelles, Belgique

Received: March 15, 2004; In Final Form: July 10, 2004

The aim of this paper is to demonstrate the importance of providing time-resolved information in catalysis research. Two truly in situ methods will be presented and compared for their merits and drawbacks: chemical transient kinetics (CTK) and pulsed field desorption mass spectrometry (PFDMS). The presentation will be given by way of example choosing the syngas (CO/H_2) reaction over cobalt-based catalysts as a catalytic process. Despite numerous efforts in the past, the mechanism of this reaction is still under debate. In CTK the reaction is studied on a metal-supported catalyst under flow conditions in a pressure range extending from atmospheric pressure down to 100 Pa. Sudden changes in the partial pressures of the reactants then allow following the relaxation to either steady-state conditions ("transients") or cleanoff ("back transients"). In PFDMS short field pulses of several volts per nanometer are applied to a model catalyst which resembles a single metal particle grain (a "tip"). These pulses intervene during the ongoing reaction under flow conditions at pressures ranging from 10^{-1} to 10^{-5} Pa and cause field desorption of adsorbed species. This method is particularly suited to detect reaction intermediates in a time-dependent manner since the repetition frequency of the pulses can be systematically varied. It is shown that both methods lead to complementary results. While CTK allows conclusions on the mechanism of CO hydrogenation by following the time-dependent formation of hydrocarbon species, PFDMS provides insight into the initial steps leading to adsorbed C_xH_y species. A quantitative assessment of the CTK data allows the demonstration that the catalyst under working conditions is in an oxidized rather than metallic state. The initial steps to oxidation are also traced by PFDMS. Most importantly, however, CTK results allow formulation of a reaction mechanism that is common for both hydrocarbon and oxygenate formation and is based on the occurrence of a formate-type species as the most abundant surface intermediate.

1. Introduction

One of the major endeavors in heterogeneous catalysis concerns the elucidation of mechanisms, kinetics, and the very nature of the active surface. Ultimately, one would like to identify the individual steps and determine their rate parameters during the ongoing catalytic reaction. There is no doubt that truly in situ experimental methods are required to meet this challenging objective. Consensus has also been reached over the past years that an analysis of the steady-state kinetics will most probably be corroborative rather than conclusive and that a detailed kinetic analysis along with the identification of "bottlenecks" or "spectators" can only be provided by applying transient methods. This has already been pointed out early on by M. Boudart,[1,2] one of the "Grands Seigneurs" in the field of kinetic research in heterogeneous catalysis.

The application of transient methods to heterogeneous catalysis began with the work of C. Wagner.[3] Later, in 1964, K. Tamaru[4] set forth the basic concepts of transient kinetics and emphasized the importance of measuring the amount of adsorption under working conditions of the catalyst. In the same paper, he pointed out that the surface composition of the catalyst changes considerably during the period of time after a fresh catalyst is brought into contact with the gaseous reactants.

A number of reviews[5−10] on dynamic transient studies have appeared in the literature during past years (see, for example, the excellent work by K. Tamaru[9]). The principles underlying step or pulse forcing of reactant pressures and catalyst temperatures have more recently also been summarized by C. O. Bennett.[10]

Transient studies of the CO hydrogenation reaction over metal-supported catalysts have frequently addressed the mechanisms and kinetics of methane formation. Steady-state isotope tracing has been employed; i.e., $^{12}CO/H_2$ gas mixtures have been abruptly replaced by either $^{13}CO/H_2$ or CO/D_2.[11−21] Various forms of carbon in either active or spectator form have been advocated to populate the catalyst surface during the reaction.[21,22] Krishna and Bell, in a steady-state tracing study of the chain lengthening on Ru/TiO_2, have suggested a reaction scheme in accordance with the Anderson−Schulz−Flory distribution of products.[21] In this scheme the chemical nature of the monomer remained unclear.

We are not aware of previous studies in which the chemical transient kinetics method (CTK) was applied to study chain lengthening in CO hydrogenation. This is surprising since after careful calibration this method allows monitoring in a quantitative manner how the reaction runs into the steady state. Furthermore, conclusions can be drawn on how the chemical state of the catalyst changes during this run-in period. In the

† Part of the special issue "Michel Boudart Festschrift".

10.1021/jp048834h CCC: $30.25
Published on Web 09/23/2004

present paper, these issues will be developed for CoCu-based catalysts that have been demonstrated to be highly selective in the production of long-chain alcohols from CO/H_2 at high pressure.[23]

Relaxation-type methods can also be designed to monitor a catalytic reaction under surface science conditions. Following the concepts introduced by M. Eigen,[24] electric field pulses can be produced in a repetitive manner to disturb the reaction on a single-crystal surface. A "frequency response" can be realized if the field pulses are strong enough to ensure field desorption of adsorbed species. The respective ions can then be detected by time-of-flight mass spectrometry. Müller et al. have been the first to describe an "atom-probe" device in which a chemical analysis is achieved by field pulses on a surface area comprising a few atoms only.[25] If a feed is leaked at a constant rate into the apparatus (while pumping at a constant rate), a "catalytic atom probe" can be constructed.[26] The method—also known as pulsed field desorption mass spectrometry (PFDMS)—can, however, only be applied under model conditions. Gas pressures are by several orders of magnitude below atmospheric, and the single crystal is given the form of a nearly hemispherical metal particle (the "model catalyst") free from any nonconducting support material. Since field pulses intervene directly during the ongoing catalytic reaction, intermediate species may be detected and analyzed as a function of the reaction time. In this manner the time period associated with the run-in to steady-state conditions is accessible.

In the present contribution, the PFDMS method is applied to study CO hydrogenation on a Co model catalyst. We also demonstrate that chemical transients kinetics (CTK) and pulsed field desorption mass spectrometry (PFDMS) may complement each other to provide a more complete picture of the reaction mechanisms and the chemical composition of the catalyst surface underlying the CO hydrogenation in different pressure regimes.

2. Experimental Section

2.1. General. Since the experimental methods applied in the present paper are quite different from each other, we start by making some general comments on the operating principles either in common or at variance.

Chemical transients on real catalysts (powders) are largely limited to pressure forcing. Constraints in the heat transport usually make it difficult to produce well-defined jumps in the temperature. This is different in single-crystal work where overall low pressures ensure molecular flow and temperatures may be increased quite rapidly by resistive heating. Unfortunately, there are kinetic and thermodynamic constraints for most catalytic synthesis reactions under net vacuum conditions. Field pulse forcing is restricted to overall pressures of $\leq 2 \times 10^{-1}$ Pa and cannot fill the pressure gap up to atmospheric conditions.

Chemical transients of the present study have been conducted by rapidly changing the partial pressure of one of the reactants. Used flow rates are associated with both the geometry of the reactor and the connecting in−out pipes. Care is taken (i) to ensure a plug-flow behavior in the pipes during transients and avoid changes in the gas-phase composition between the outlet of the reactor and the analytical device and (ii) to ensure a well-mixed reactor. Such a gradientless environment is a necessary condition if we want to obtain a uniform surface composition in the catalytic bed. This is important if correlations have to be made between catalytic properties and coverages during their variation in the course of a transient experiment.

When using field pulses in relaxation studies with three-dimensional (3D) single crystals, gas fluxes and partial pressures of reactants remain constant at any time. Pulses intervene during the ongoing reaction to (i) cause field desorption of the adsorbed layer. Respective ions follow the gradient of the electric field and move collision-free to an analytical device with single-particle sensitivity. Pulses also intervene to (ii) define a new reaction time period with starting conditions varying between zero and steady-state coverage (corresponding to field desorption with complete and, respectively, negligible layer removal).

Both methods, CTK and PFDMS, can be calibrated to allow quantification. Quite importantly, following the above arguments, CTK allows the average surface composition to be evaluated from an in−out mass balance during transients. In fact, to calculate the change of moles in the gas phase as a function of time, the variation of the partial pressure with time is measured for each species while keeping constant the influx. Differently from many other studies (see, for example, the work by F. Margitfalvi[27,28] on hydrogenolysis), the outflux is also followed with time so that the net adsorption rate, $r_{des} - r_{ads}$, becomes accessible. In refs 27 and 28 the reactor was not mixed and thus no useful value of the surface coverage could be derived.

Due to variations of the catalyst activity while performing transients, variations of the volumetric flow rate have to be expected. This is taken into account by using an inert internal standard[29] (Ar, Ne, He, ...), the partial pressure of which is inversely proportional to the volumetric flow rate.

Quantification in PFDMS can only be achieved if field pulses cause complete desorption of adsorbed layers. In that case, ion intensities reflect surface coverages; the latter can be calculated provided the size of the monitored surface area is known.

Samples used in both methods are quite different. While real catalysts in the form of powders are used in CTK, a single crystal is taken in PFDMS. Thus a pore texture with a certain particle size distribution is existent on one hand, whereas a single metal grain is present on the other. There is no doubt that the "single-grain approach" in PFDMS is another manifestation of the "material gap": despite a well-defined 3D sample morphology (comprising surface planes and sites that can even be made visible by field ion microscopy; see below), there is no means to take into account possible metal−(ceramic) support interactions in PFDMS. With this drawback, possible time-dependent changes in the size and distribution of metal particles on a support cannot be addressed with this method. However, morphological changes of metal particles can be imaged with atomic resolution by operating the PFDMS apparatus in the FIM mode (field ion microscopy). We mention that surface areas of powder samples can be easily measured by BET at any time in the CTK apparatus once the volumetric outflow has been determined.[29]

2.2. Experimental Details of the CKT Method, Apparatus, and Catalysts. The reactor is of Pyrex with an inner diameter of ~1 cm and a volume of ~1 cm^3. The catalyst is deposited on a Pyrex frit inside the reactor. The porosity of the frit is adapted to the grain size of the catalyst. The reactor is surrounded by a homemade air thermostat.

Transient measurements are performed at atmospheric pressures. Small amounts of an inert gas are added to the reactants as an internal standard. This allows taking into account variations of the volumetric flow rate as mentioned above. Volumetric flow rates are in the range 0.3−1.0 $cm^3 \cdot s^{-1}$. The experimental setup used in our measurements can be seen in Figure 1. We mention that the valves are not operated choked as in a TAP apparatus (temporal analysis of products). The time response in transient measurements is largely limited by the

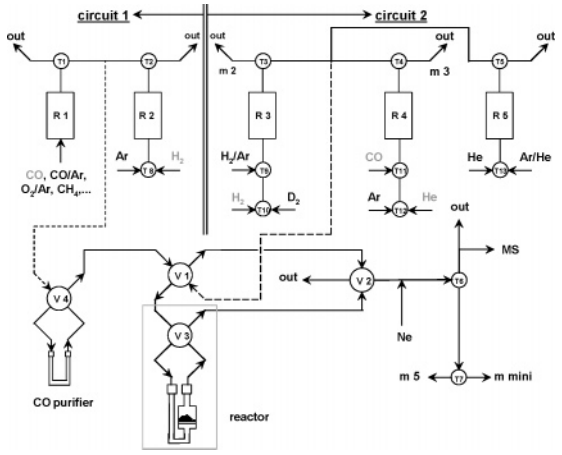

Figure 1. Scheme of the apparatus used for the measurement of chemical transient kinetics.

presence of a dead volume which cannot be avoided in a TAP instrument either.

Four-way valve V3 allows the gas-phase composition to be changed abruptly. The achievement of a well-mixed reactor is checked by replacing a flux of carbon monoxide by a flux of argon and using a catalytically inert material (such as SiC). This results in an exponential decay of the pressure with a time constant characteristic of the dead volume of the reactor.

CoCu-based catalysts are prepared following the oxalate coprecipitation method developed in our laboratory. In most catalysts of the present study, Mg (also coprecipitated into an oxalate form) has been used as a dispersant. The preparation and characterization of the catalysts are described elsewhere.[30,31] The gas composition is continuously analyzed at the outlet of the reactor by means of a differentially pumped quadrupole mass spectrometer (Balzers QMG 420).

2.3. Experimental Details of the PFDMS Method and Apparatus. The PFDMS (pulsed field desorption mass spectrometry) setup is based on a combination of field ion microscopy and "atom-probe" time-of-flight mass spectrometry. Figure 2 shows a typical field ion micrograph along with a ball model of the nearly spherical model catalyst ("field emitter tip") and the principle of the atom-probe technique. One can clearly recognize a number of different surface planes which usually exhibit different catalytic activity (left). Chemical probing of the catalyst surface is achieved via a small hole in an electrode ($\phi \sim 1$ mm) placed in front of the model catalyst. High electric field strengths, $F < 40$ V/nm, are produced in the form of short negative field pulses (widths $\sim$ 100 ns, repetition rates $\leq$ 10 kHz) at this counter electrode in order to cause field desorption of the adsorbed layer. Respective ions are subsequently mass-separated in a time-of-flight tube as described in detail elsewhere.[32] The instrument is run as a flow reactor at overall low pressures ($\leq 2 \times 10^{-2}$ Pa). The size of the monitored area can be varied by means of an electrostatic lens located in the time-of-flight tube (not shown). Usually, lens settings are used that allow areas with some ten to a few hundred atomic sites to be probed by field pulses.

Co specimens are prepared by electrochemical etching of a thin ($\phi = 0.1$ mm) Co wire in $CH_3COOH/HClO_4$ (20:1).

2.4. Kinetic Measurements with the PFDMS Method. As compared to CTK, PFDMS is much less widespread as a method to provide information on the mechanism and kinetics of catalytic reactions. Thus we present here some of the clues of its operation principles.

Qualitative insight into the surface layer composition is obtained by using low-amplitude field pulses. Under these

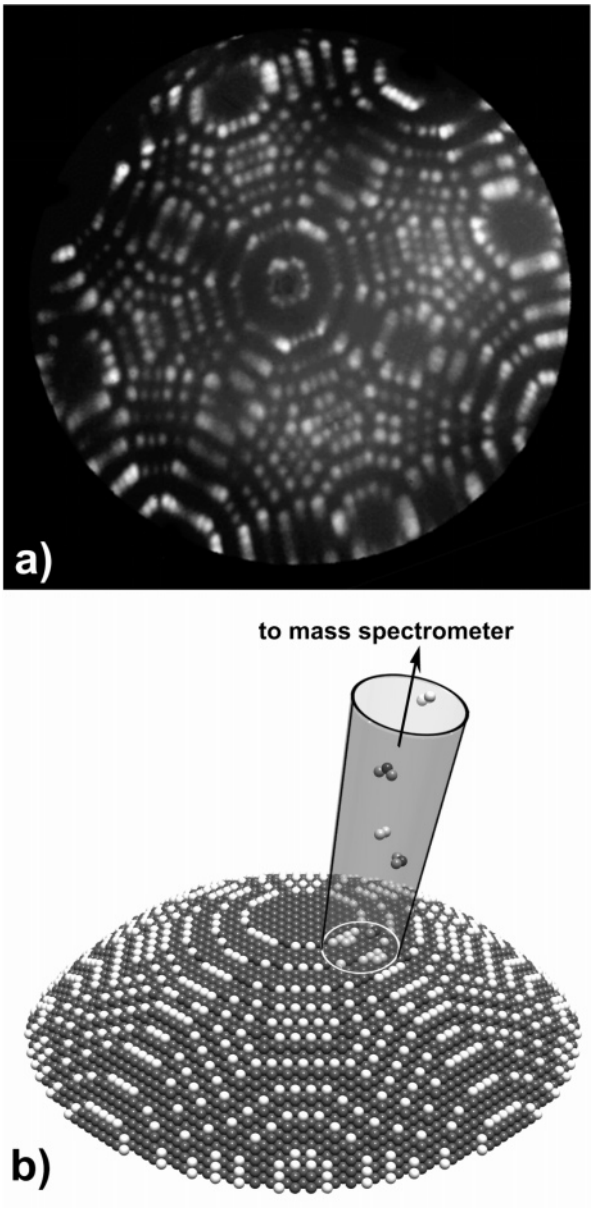

Figure 2. (a) Field ion micrograph of a (001)-oriented fcc crystal at best image condions in Ne (radius of the tip $\sim$10 nm) along with a ball model (b) demonstrating the suitability of the crystal morphology (the tip or "model catalyst") for catalysis research. Various different surface planes are simultaneously exposed and can be probed by relaxation mass spectroscopy for their catalytic activity.

conditions the layer composition is nearly constant throughout the measurements: small amounts removed by pulses are immediately refilled by adsorption between pulses. The identification of true surface species is not straightforward under these conditions unless patterns of species fragmentation or association are known. Quite generally, assignments can be facilitated through temperature and pressure variation. However, the PFDMS method also allows study of the influence of the electric field strength through independent variation of the field pulse amplitude and the dc field. This procedure has been recently applied to reveal the field-promoted carbonyl formation on gold surfaces.[33]

In Figure 3 the general experimental procedure for kinetic measurements is illustrated. Adsorption takes place during t_R, while gaseous reactants impinge on the surface. A dc field may be applied arbitrarily. The field pulses stop the adsorption process and cause desorption of the adsorbed layer. Provided

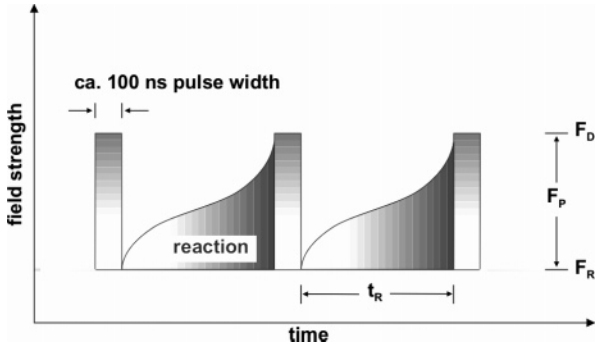

Figure 3. Time scheme of the field pulses leading to field desorption after a reaction interval t_R between pulses. An electric dc field, F_R, can be additionally applied. F_D = total desorption field strength; F_P = pulsed field strength.

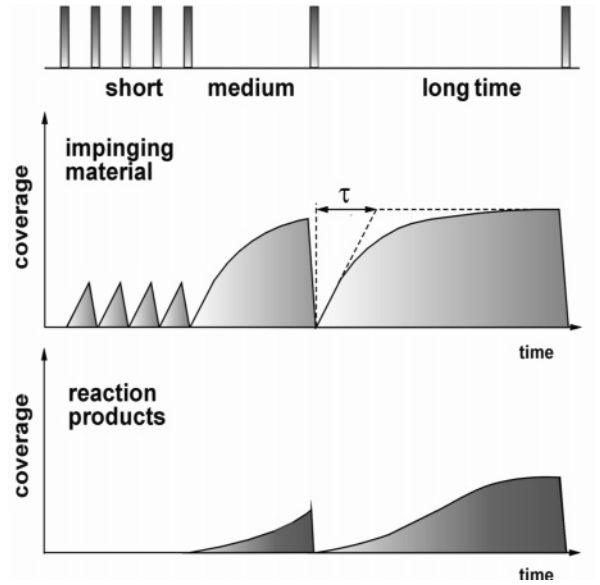

Figure 4. Scheme illustrating field pulses of a certain repetition frequency. A systematic variation of the reaction time, t_R, provides kinetic information.

the layer removal is complete with each pulse, the ion intensity, i.e., the number of ions detected with each pulse (ions per pulse), is a measure of the surface coverage built up within the monitored area between any two pulses.

Kinetic data of surface reactions can be obtained by varying the repetition rate, i.e., the reaction time t_R between the field pulses. This is usually done by scanning the range from 100 μs up to some seconds (in fact, there is no limitation to the "long end"). Three different pulse repetition rates, corresponding to short, medium, and long field-free times t_R, are depicted in Figure 4. For short times, as indicated on the left-hand side of the figure, the surface coverage that can be reached by adsorption during t_R is far below the monolayer limit. Only the initial stages of adsorption are monitored under these conditions. Usually t_R has to be increased to allow surface reactions to be initiated. At medium t_R, field pulses will detect intermediate species, while at long times the surface reaction may run into a steady state so that products appear in the mass spectra. Alternatively, depending on temperature and pressure, the surface coverage may also reach saturation. In fact, severe site blocking may occur if the partial pressures of reactants are not properly adjusted. Such a case will be demonstrated later on for the CO hydrogenation on Co model catalysts.

3. Results

The Results section of this paper is organized in the following manner. We begin by presenting data on the CO hydrogenation over CoCu-based catalysts using CTK. For principal reasons (CoCu alloys do not exist!), Co model catalysts are investigated by PFDMS. Respective data will be presented subsequently.

3.1. CO Hydrogenation over CoCu-Based Catalysts: Studies by CTK. The motivation to use CTK in studies of the CO hydrogenation is (i) to provide information during the transient period for the "as-prepared" catalyst to adapt to the reaction gas phase and to follow simultaneously (ia) variations of the kinetics (adsorption of reactants, appearance of products, and desorption) and (ib) values and variations of the coverage. This will allow establishment of correlations between coverage and kinetics. Other motivations to use CTK in studies of CO hydrogenation are (ii) to try to determine the chemical state of the catalyst surface under catalytic working conditions and (iii) to obtain direct evidence concerning the nature of the monomer involved in the Fischer−Tropsch synthesis.

The mechanism of the catalytic CO−H_2 reaction is still much under debate. The unique capabilities of the CTK method allow providing new insight into the mechanism over CoCu-based catalysts.

We start by describing surface buildup and cleanoff through measurements of chemical transients in the forward and backward reaction, respectively. Accordingly, after reaching constant temperatures and steady H_2 flux over the CoCu catalyst, a transient experiment is started by producing a step function of the CO partial pressure. Experimentally, this is done by switching valve V1 in Figure 1 to replace a given flux of an inert gas (He in this case) by the same flux of CO. After reaching the steady-state catalytic activity the procedure is reversed while all other parameters are kept constant (surface cleanoff or back transient).

3.1.1. Buildup Transient. A typical buildup transient is shown in Figure 5a. The experiment is conducted at 280 °C, on a CoCuMg catalyst (1−1−2.5 in atoms) of 0.3 g. The active surface area is associated with a chemisorption capacity for CO at room temperature which equals 90×10^{19} CO molecules g^{-1} of Co metal. Switching the inlet from He to CO with the same flux takes place after 50 s. At the same time the CO pressure should increase according to the dotted curve calculated from the He decrease. In practice, during nearly 15 s no CO appears in the gas phase; it is quantitatively consumed by the catalyst. The total "flux out" thus decreases, inducing a drop of the volumetric flow rate. The variations of the volumetric flow rate may be measured continuously by an original method using an internal standard (here neon) and published previously.[29] This appears clearly on the variation of the partial pressure of argon. Similarly, an increase of the partial pressure of H_2 is observed. Nevertheless, the increase in H_2 pressure is lower than the one expected from the lowering of the volumetric flow rate; thus some H_2 is consumed. In fact, Figure 6 shows the importance of the variation of the volumetric flow rate during the transient period. It is then possible to calculate the flux in moles per second for all species. Figure 6 also indicates that, despite a positive peak in the H_2 pressure being observed, a negative peak corresponding to the consumption of H_2 is calculated. Applying a similar procedure to the carbon- and oxygen-containing molecules allows then calculation of a balance of species (carbon and oxygen) during the transient. The corresponding results appear in Figure 7. Let us also mention that the abscissa in Figure 5a extends up to 300 s to show that after 200 s steady-state activity is attained.

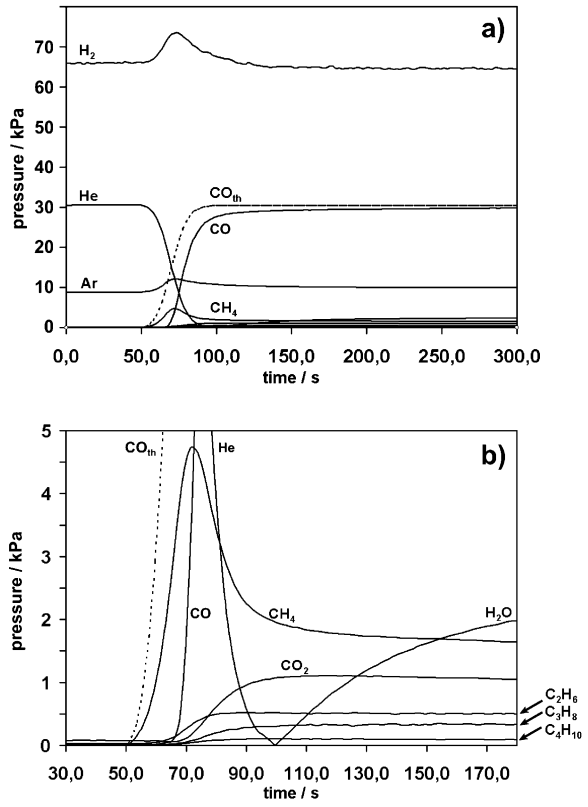

Figure 5. (a) Variation of the partial pressure as measured by the quadrupole mass spectrometer in the gas flow at the outlet of the reactor during a buildup transient on a CoCu-based catalyst at 280 °C. (b) Zoom into the period of time in Figure 5a where the most significant changes in the partial pressures of the reaction products occur during a buildup transient.

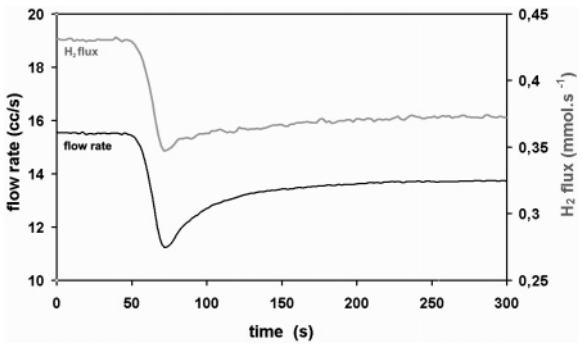

Figure 6. Bottom curve: Variation of the volumetric flow rate during the transient buildup as derived from the variation of the partial pressure of argon used as internal standard. Top curve: Variation of the flux of H_2 at the outlet of the reactor during the buildup transient. Same catalyst and temperature as in Figure 5.

To improve the visibility of details in the period between 50 and 100 s, the results in this range are zoomed in in Figure 5b.

If no CO appears in the gas phase before 15 s, at the time CO is introduced, part of the carbon brought to the surface in the form of CO is desorbed in the form of CH_4. This explains the consumption of H_2. During this 15 s, only CH_4 leaves the surface. It is remarkable that ethane starts to appear in the gas phase at the same time as CO. Nearly at the same time CO_2 also starts to appear. The CO pressure continues to increase sharply and the production of CH_4 goes through a maximum, whereas the production of CO_2 reaches a steady value. The production of C_3 and C_4 hydrocarbons follows in sequence.

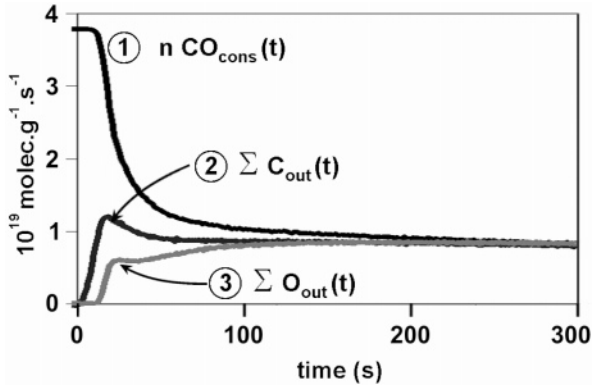

Figure 7. Instant in−out mass balance during the transient. Curve 1: adsorption of CO. Curves 2 and 3: total amount of C and of O atoms in all compounds liberated from the surface of the catalyst. Same catalyst and temperature as in Figure 5.

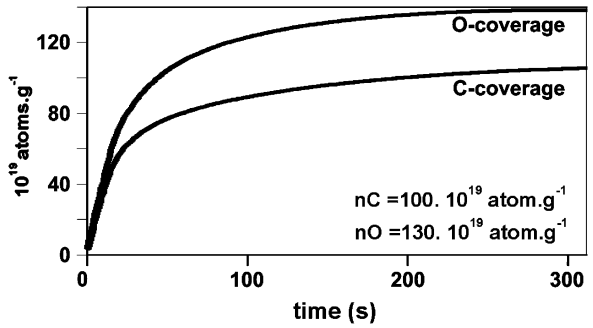

Figure 8. Buildup of the average surface coverages of O and C atoms during the buildup transient. Values are calculated from integrated in−out mass balances. Data refer to a CoCu-based catalyst at 280 °C and pressure conditions as defined in Figure 5.

Water production starts only after all the carbon-containing species have reached the steady state. It needs over 250 s to reach a steady production rate.

Comparison between Figures 5a and 7 shows that the catalytic activity reaches the steady state at the same time as the coverage. By integration of the instant in−out balance, it is possible to obtain the coverage and its variations with time as presented in Figure 8. The results may be expressed not only as a function of time but also as a function of coverage. At steady activity the production of the sequence of produced hydrocarbons obeys the Anderson−Schulz−Flory (ASF) distribution.[34] In the presented example the α_{ASF} value is ~0.43.

3.1.2. Back Transient. After reaching the steady state, a "back transient" is started by switching V1 (see Figure 1) from CO to He. The results are presented in Figure 9. For each species, the data are presented in the form of the pressure normalized to its value during the steady regime of activity. For He, the values plotted correspond to $p_{stat} - p(t)$.

Four different patterns of behavior are observed for the desorption of the various species from the surface:

(i) CO: Its partial pressure decreases in the same way as that for He ($p_{stat} - p(t)$).

(ii) CO_2 and C_{2+}: The values characteristic of all hydrocarbons (HC) containing two or more C atoms as well as those of CO_2 decrease with the same time dependence. This is in agreement with the observed ASF distribution of the steady state.

(iii) H_2O: Water leaves the surface much more slowly, but decreases monotonically from the steady-state value. Delays longer than 200 s are necessary to eliminate all the oxygen in form of H_2O.

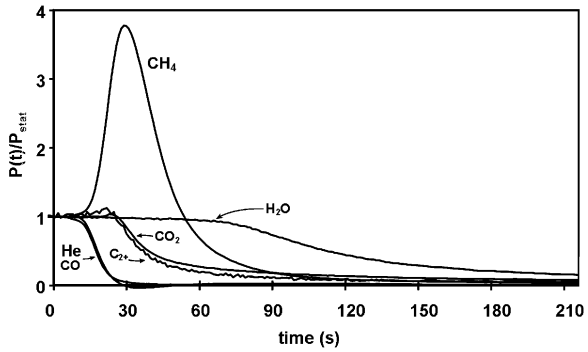

Figure 9. Back transient following the steady state reached at the end of Figure 5a. Here the results are expressed in terms of normalized pressures with respect to the values at steady state.

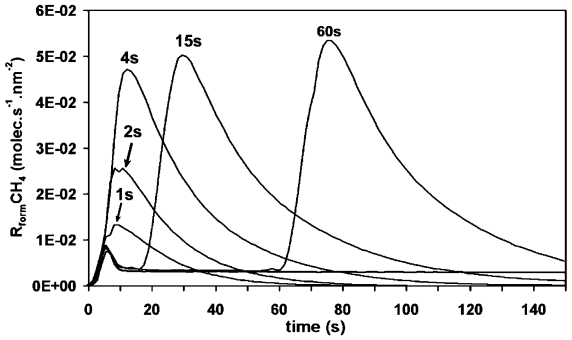

Figure 10. Buildup and back transients following CO inlet pulses of different duration on a CoCu-based catalyst at 280 °C.

(iv) CH_4: Methane exhibits a completely different behavior. Its production increases remarkably and reaches a maximum before going down to negligible values.

Let us mention here that if instead of replacing the inlet of CO by He one replaces the total "flux in" (CO + H_2) by He, no surface cleanoff is seen. This clearly indicates the important role of H_2 in the mechanism of desorption.[34]

3.1.3. Pulses. The results presented in this subsection correspond to experiments conducted under exactly the same conditions as standard CTK exposed above except for the introduction of CO which is managed in a pulsed manner rather than stepwise to induce buildup or cleanoff; that is, the inlet of CO lasts for a given period of time.

In Figure 10, only methane formation is plotted. Both classical transient behavior (curve indicated by the arrow) and a series of pulses of different duration are presented. One can first see that, in the classical transient, steady-state production of CH_4 is attained after ∼10 s. On pulses of 60 and 15 s duration, the same steady value of methane production rate is attained. The shape and amplitude of the first peak (at 6 s) are the same as in the standard transient experiment.

The two peaks corresponding to inlet periods of 1 and 2 s present a very different shape. Only one single peak is observed, the integral of which provides values of coverages in the range of only 10−20% of that attained at steady state. Deeper insight into the kinetics under pulse conditions might be expected by working at lower temperatures, or in a lower pressure range to render possible quantitative comparison with results obtained by PFDMS.

3.2. CO Hydrogenation over Co Model Catalysts: the Studies by PFDMS. The PFDMS method has been applied to study both the adsorption of CO and the reaction of CO with hydrogen on a Co tip specimen. Major incentives for this study are (i) to provide evidence for the formation of Co carbonyl species which have recently been considered to be involved in the restructuring of Co surfaces,[36] (ii) to provide kinetic insight into the CO decomposition with subsequent buildup of carbidic and oxydic phases, (iii) to demonstrate mechanistic pathways during the very initial stages of hydrocarbon formation from CO and hydrogen, and (iv) to reveal site-blocking effects during CO hydrogenation at overall low gas pressures and insufficient H_2 partial pressures.

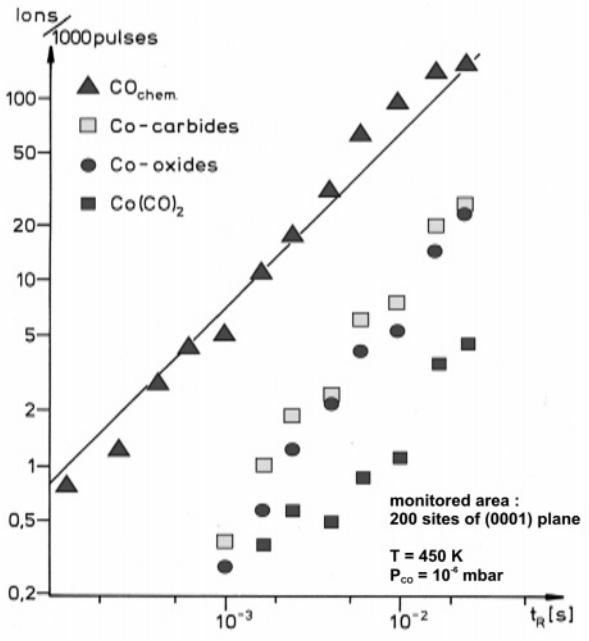

Figure 11. Time dependence of ion intensities detected during CO reaction with a Co tip (the model catalyst) at 450 K, $P_{CO} = 1.3 \times 10^{-3}$ Pa, and ∼30 V/nm. No steady electric field is applied.

Turning to (i) and (ii), a $(10\bar{1}0)$-oriented Co tip has been continuously exposed to CO gas at a pressure of 1.3×10^{-4} Pa and 450 K. Using the probe hole technique, ∼200 atomic sites of the (0001) plane are monitored by field pulses of an amplitude close to 30 V/nm. Under these conditions complete field desorption of the adsorbed layer is achieved so that the species intensities reflect surface coverages. Separate experiments with varying field strengths (not shown here) have indeed demonstrated that quantitative field desorption is achieved at field strengths above 28 V/nm. Under these conditions considerable amounts of field evaporated Co^+ and Co^{2+} species appear in the mass spectra (which leads to a rapid layer-by-layer "consumption" of the catalyst).

The mass spectra acquired under the above conditions are quite "rich" and contain a variety of different species. Quite generally we can distinguish between molecular CO adsorption, association in terms of subcarbonyl formation, and decomposition. Both CO^+ and $CoCO^+$ species are representative of molecular CO adsorption. For energetic reasons of ion formation, $CoCO^+$ is considered to field evaporate as intact surface complex from step or kink sites. Co subcarbonyls, $Co(CO)_x^+$ ($x = 2, 3$), indicate that part of the chemisorbed CO may associate in "twins" or "triplets". Again, for energetic (but also for steric) reasons such multiply bound CO most probably involves Co step (kink) atoms. Dissociative adsorption of CO leads to the buildup of oxidic and carbidic phases which are field desorbed in the form of Co_2O^{2+}, CoO^+, CoC^+, and CoC_2^+ species. Smaller amounts of C^{2+}, C^+, and C_2^+ are also seen in the spectra.

In Figure 11 the ion intensities are plotted as a function of the reaction time under field conditions leading to quantitative

desorption. It is seen that the surface coverage of chemisorbed CO (the sum of CO^+ and $CoCO^+$) increases linearly with time. Indeed, a Langmuir behavior with high sticking probability is expected since the total surface coverage always remains far below the monolayer limit for the range of reaction times chosen here. Associative CO adsorption mainly runs up to $Co(CO)_2$. Respective ion intensities remain quite low, however. Higher subcarbonyl homologues ($Co(CO)_3$ in particular) occur with even larger statistical fluctuations and have been omitted in Figure 11.

Particular interest concerns the buildup of carbidic and oxidic phases. According to Figure 11 (the sum of Co_2O^{2+}, CoO^+ and of C^{2+}, C^+, C_2^+, CoC^+, CoC_2^+ intensities are represented) a process of higher kinetic order, $d\ln(\theta)/d\ln(t_R) \sim 2$, is in operation. In fact, this finding is in agreement with a consecutive reaction model in which molecular CO adsorption occurs first and dissociation successively. It might be suspected that CO dissociation and subcarbonyl formation are competitive processes on our Co model catalyst: both are likely to involve steps and kinks. At 450 K the dissociation process seems to dominate, and we suggest that this is the reason for the relatively low $Co(CO)_x$ intensities. Previous measurements on Ni carbonylation have also demonstrated that site-blocking effects due to carbon deposition may occur.[37]

Surface coverages in Figure 11 remain low. Assuming high CO sticking probabilities—a value of 0.9 was reported for the Co (0001) surface[36]—the highest values reached are about 1% of a monolayer. Thus our Co model catalyst may be considered to be in a "metallic" state within the range of measured reaction times. If an extrapolation is made to $t_R \geq 20$ ms, we expect the surface coverages of carbon and oxygen to be similar to those of molecular CO at $t_R \sim 0.2$ s. It is most probable that the CO sticking probability decreases while further increasing t_R.

We next discuss PFDMS data on the early stages of hydrocarbon formation while dosing the Co model catalyst with a mixture of CO and hydrogen. Figure 12 compares respective time-of-flight mass spectra obtained at a reaction time of 1 ms (top) and 1 s (bottom) at otherwise constant reaction conditions: $p_{tot} = 10^{-1}$ Pa, $p_{H_2}/p_{CO} = 2$, and $T = 500$ K. Again, the field strength has been adjusted such that quantitative field desorption is achieved. Large quantities of Co^+ and Co^{2+} (the most abundant species with absolute numbers of several thousand ions in each spectrum) are formed under these conditions. As expected, considerable amounts of carbidic and oxidic species build up during the field-free (no dc field) reaction times. Particular interest concerns the occurrence of ionic CH_x species, the neutrals of which can be considered reactive intermediates of the methanation reaction. The occurrence of C^+, CH^+, and CH_2^+ in the top spectrum indicates surface carbon reacts with hydrogen in a stepwise manner up to $CH_{2,ad}$ during $t_R = 1$ ms. Increasing the reaction time to 1 s (bottom spectrum) probably leads to methane production. This is indicated by the additional appearance of CH_3^+ species in the respective mass spectrum. The reaction product, CH_4, undergoes thermal desorption and thus escapes detection by field pulses. The concomitant formation of water, which is desorbed as H_2O^+ or H_3O^+, may be considered another indication that methane forms under the chosen reaction conditions.

Quite interestingly, subcarbonyl species, $Co(CO)_x$, are also formed during CO hydrogenation. Such species have previously been considered to be involved in the restructuring of Co model catalysts.[31,36] Following CO hydrogenation at 0.4 MPa and 520 K on a flat Co(0001) single crystal, scanning tunneling microscopy (STM) demonstrated roughening of the initially flat surface along with homogeneous island formation. An etch−regrowth mechanism mediated by surface transport of Co atoms, possibly in the form of carbonyls, was considered. The present PFDMS study proves that Co subcarbonyls are indeed formed. In addition to that, extensive studies of carbonyl formation on metals such as Ni, Rh, or Ru[39−41] have demonstrated such carbonyl species to be mobile and likely involved in morphological shape transformations. Future studies by PFDMS will address the question for $Co(CO)_{x,ad}$ mobility. The data material presently at hand does not yet allow definitive conclusions on that issue.

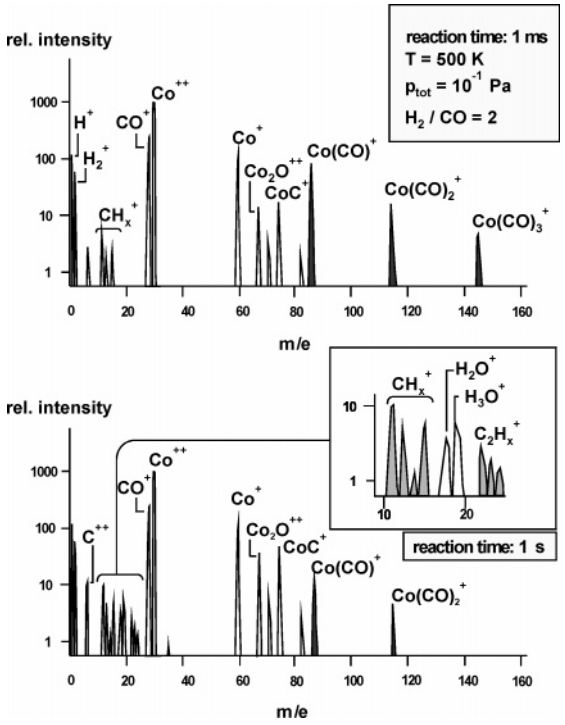

Figure 12. Relative ion intensities during CO hydrogenation on Co at short time $t_R = 1$ ms and long time $t_R = 1$ s. Experimental conditions as indicated in the insert. The field strength is high (close to 30 V/nm) to ensure quantitative desorption and kinetic conditions without inhibition effects.

We finally turn to a steady layer analysis while dosing the Co model catalyst at 405 K and $p_{tot} = 4 \times 10^{-2}$ Pa ($p_{H_2}/p_{CO} = 2$). To render possible this analysis, field pulses of moderate amplitude, $F_D = 25$ V/nm, have been employed. Under these conditions field desorbed amounts are immediately refilled by adsorption between pulses. The results, shown in Figure 13, are presented in the form of a time-of-flight spectrum (in fact, several spectra with different pulse repetition frequencies have been summed and normalized to the intensity of Co^{2+}, which is the most abundant species). As compared to Figure 12, $C_xH_y^+$ ($x = 1-4$, $y \leq 3$) rather than Co carbides or oxides occur. Thus $Co-C_x$ bonds rather than $Co-CoC_x$ bonds are broken. Moreover, no Co subcarbonyls, $Co(CO)_x^+$, are detected. It must be concluded that the surface composition is dominated by carbon species which accumulate with time (due to incomplete field desorption) and react partially with adsorbed hydrogen. Possibly step sites are pinned by carbon species so that Co subcarbonyl formation is prevented.

4. Discussion

The CTK method has been applied in the atmospheric pressure range. As already argued earlier,[42] the time response to pressure forcing varies in an inverse manner with the total

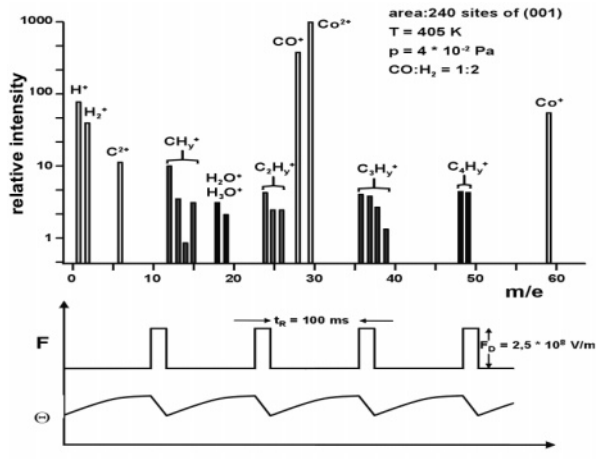

Figure 13. Relative ion intensities during CO hydrogenation on Co at 405 K, $p = 4 \times 10^{-2}$ Pa, CO:H_2 = 1:2, and $F_D = F_P = 25$ V/nm. A mean-value spectrum is constructed from individual spectra taken under field strength conditions insufficient to ensure complete desorption.

pressure. As seen in the Results section, the total transient period is in the range 10−100 s. Due to specific experimental conditions (volume of the reactor, volumetric flow rate), the time constant characteristic of the dead volume is in the range of 1 s. Furthermore, the quadrupole mass spectrometer used for the measurements has an analysis frequency of one spectrum per second. This means that working at pressures much higher than atmospheric will hardly be possible with our system.

The range of reaction times accessible in PFDMS is much lower than in CTK. Since the reactant pressures are by orders of magnitude below those in CTK, the surface coverages reached in PFDMS frequently remain at a fraction of a monolayer. Broadly speaking, this has a negative influence on reaction probabilities.

Regarding hydrocarbon formation from CO/H_2 mixtures, CH_{ad} species have been detected as precursors of the methane production on Co 3D model catalysts. Reaction times in the millisecond range have been measured at 10^{-1} Pa and 500 K. Chain lengthening may be observed in PFDMS; however, C_x species do not hydrogenate easily at low hydrogen partial pressures. Instead, surface carbon accumulates on the surface. This is a clear manifestation of the pressure gap problem. Before turning to the detailed mechanistic and kinetic evidence associated with hydrocarbon formation on CoCu-based catalysts, we mention (without experimental proof) that the importance of sufficient hydrogen partial pressures has already been demonstrated in CTK:[35] lowering the total pressure from atmospheric pressure to the millibar region at otherwise constant CO/H_2 partial pressure ratio obviously causes the reaction to redirect to CO_2 and CH_4 with negligible water production.

The CO hydrogenation over CoCu-based catalysts has been extensively studied in two recent Ph.D. theses,[43,44] which both suggest a reaction mechanism involving only one type of site for the production of both oxygenates and hydrocarbons in the high-pressure range ($p_{reactor} > 3$ MPa). For the production of "HC" only, as is the case in the present CTK study, this mechanism is reduced to the one presented in Figure 14. In the complete scheme presented elsewhere,[34,43,44] the surface hydrogenation comprises elementary steps producing oxygenated radicals which lead to the production of alcohols and hydrocarbons. Let us mention that, in the high-pressure range, the α_{ASF} has the same value for the production of alcohols as for hydrocarbons. This is in favor of a single reaction scheme in which a single reaction site is in operation.

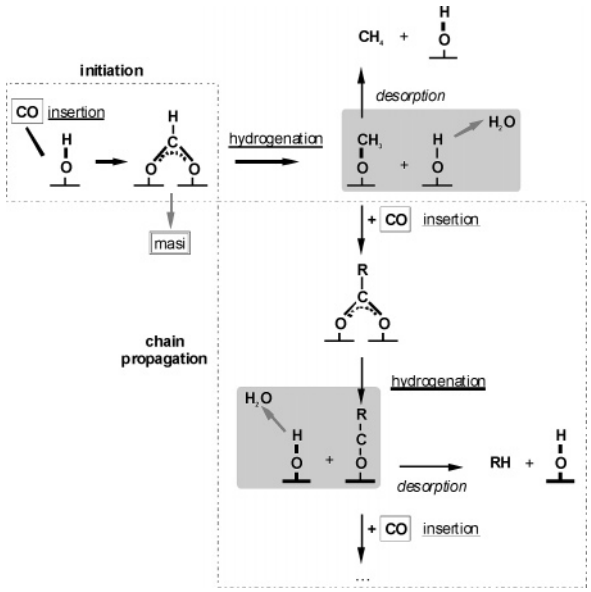

Figure 14. Proposed reaction mechanism for the CO−H_2 reaction on CoCu-based catalysts.

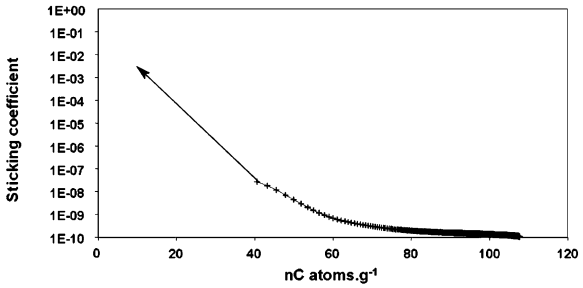

Figure 15. Variation of the calculated sticking coefficient of CO as a function of carbon coverage on a CoCu-based catalyst (derived from buildup measurements as shown in Figure 5).

The behavior of the CO partial pressure in the back transient indicates that no CO desorbs from the surface. Thus, under these conditions the adsorption of CO is nearly irreversible. From the measurements of the net adsorption rate it is possible to calculate the value of the CO sticking coefficient during catalysis. In Figure 15, the values of this sticking coefficient are plotted versus the number of surface carbon atoms during the buildup transient. For values between 10^{-7} and 10^{-6}, transport limitations in a porous material make the calculations progressively meaningless. It is interesting to note, however, that the extrapolation from values of 10^{-9} to 10^{-6} to low coverage make the sticking probability reach values between 10^{-2} and 1, which is in agreement with the values measured for CO adsorption on a nearly clean Co 3D single crystal by means of PFDMS.

Let us now discuss, in the framework of the proposed mechanism, the answers that can be given to the various questions mentioned in the Introduction:

(1) On which type of surface does the CO hydrogenation reaction take place?

The available surface is derived from the CO chemisorption capacity at room temperature. It happens that the O and C coverage reached at steady-state conditions of the working catalyst is very high as shown in Figure 8. The surface is thus no longer metallic as we consider in the mechanism (Figure 14). Furthermore, Figure 5 indicates that the selectivity properties change considerably with the coverage.

The change of the surface from metallic to carbon and oxygen covered is also demonstrated during CO interaction with a Co

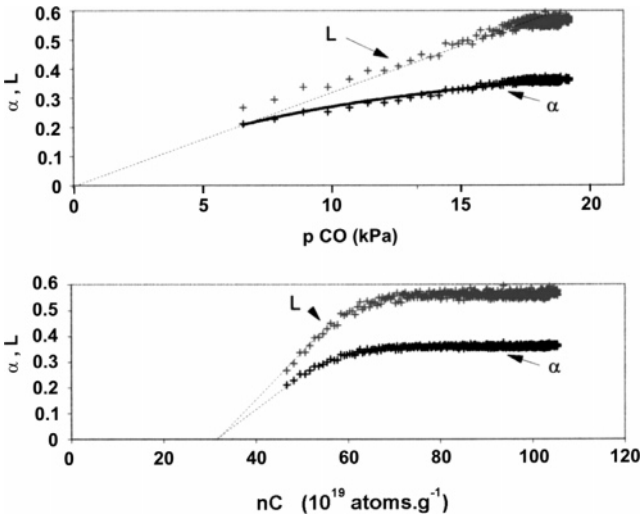

Figure 16. (a, top) Variation of the distribution of products during the buildup transient of Figure 5 expressed as $\alpha_{ASF} = R_a/(R_a + R_{des})$ and $L = R_a/R_{des}$ plotted as a function of p_{CO}. (b, bottom) same results as in (a) but plotted as a function of the carbon coverage.

3D single crystal. PFDMS has clearly revealed that carbon and oxygen deposition follows CO adsorption. The possibility of tracing the in situ kinetics of such a process on the scale of a few surface atoms of a well-defined face is a manifestation of the power of PFDMS to provide face-selective or even site-selective data along with mechanistic insight.

(2) What is the nature of the monomer responsible for chain lengthening?[45−47]

During a back transient, the decrease in CO pressure exhibits the characteristics of the emptying of the dead volume. This leads to consideration of CO adsorption to be nearly irreversible. During the buildup transient, as long as there is no CO appearing in the gas phase, no chain lengthening is observed. Only methane leaves the surface. Furthermore, during the transient an ASF distribution of the products is observed with α_{ASF} and L values ($\alpha_{ASF} = R_a/(R_a + R_{des})$ and $L = R_a/R_{des}$) varying almost linearly with the CO pressure (Figure 16a). On the contrary, α and L variations do not exhibit any simple correlation with the carbon coverage (Figure 16b). Thus these results indicate clearly that the monomer responsible for chain lengthening is in this case CO and not a CH_x surface complex. Reciprocally, stopping the inlet of CO hinders the CO insertion and thus inhibits further reaction except desorption. All the precursors of the various hydrocarbons then desorb in accordance with one of the requirements for an ASF mechanism, i.e., the same probability for desorption whatever the chain length. This is also verified in Figure 9, where clearly the time dependence for the C_{2+} to desorb is the same for all hydrocarbons (except for CH_4). The particular behavior of methane is due to the fact that the most abundant surface intermediate (MASI) may then only undergo reduction, leading finally to CH_4 production and cease of chain lengthening.[34]

We conclude our discussion by inspecting a reaction process observed in PFDMS on Co but not in CTK (on CoCu). Under in situ reaction conditions of mere CO or mixtures of CO and hydrogen, Co subcarbonyls, $Co(CO)_x$ ($x = 2, 3$), have been detected. Such species may be involved in the restructuring of the catalyst surface during the run-in period of the catalyst. Since subcarbonyl formation is likely in competition with CO decomposition, a transient surface process must be envisaged which can only be observed using surface analytical tools of ultimate sensitivity.

Further research on Co subcarbonyl formation must be conducted to arrive at more detailed conclusions. We mention also that in the earlier literature subcarbonyls have been suggested to be the precursor species of CO insertion[48] into a growing hydrocarbon chain. While the CTK results described formerly[34,44] and in the present study also suggest CO insertion to be in operation (on primary surface complexes different from those considered by Pichler and Schulz[48]), we cannot differentiate between a carbonyl and adsorbed CO as precursor. We mention that PFDMS has provided no evidence as yet for the formation of Co carbonyls under high-coverage conditions of the CO hydrogenation.

5. General Conclusions

The main difficulties to establishing quantitative correlations obtained by the two methods presented here are probably due to the effect of very large differences in the hydrogen pressure (on the average 5−6 orders of magnitude). Difficulties due to hydrogen effects already received much attention by one of us.[35] It is clear, when looking at the time dependence of the surface species with hydrogen to react (see back transients in the CTK method), that the role of hydrogen in the 10^{-1}−10^{-5} Pa pressure range and in delays shorter than 1 s is completely negligible. On the other hand, the PFDMS method is very unique in providing time-resolved information on the initial interaction of CO with the metal surface. The information obtained on the kinetics of the oxide formation is in agreement with concepts derived at atmospheric pressure according to which catalysis proceeds, under steady conditions, on an oxidized surface and not on a bare metal surface.

The CTK method provides convincing evidence concerning the nature of the monomer responsible for chain lengthening in the Fischer−Tropsch synthesis. It has also allowed definition of the nature of the MASI.[34] Finally, combined with the results obtained at high pressure (6 MPa), it has led us to propose one single mechanism taking place on one single site demonstrating the origin of the selectivity to be purely of kinetic nature.

Acknowledgment. It is the pleasure of A.F. to take here the opportunity to express his gratitude toward Michel Boudart for so many very instructive discussions during his stay at Stanford for several years. T.V. is supported by the Fonds National de la Recherche Scientifique (FNRS), which is gratefully acknowledged.

References and Notes

(1) Boudart, M.; Djéga-Mariadassou, G. *Kinetics of Heterogeneous Catalytic Reactions*; Princeton University Press: Princeton, NJ, 1984.
(2) Boudart, M. In *Handbook of Heterogeneous Catalysis*; Ertl, G., Knözinger, H., Weitkamp, J., Eds.; Wiley-VCH: New York, 1997; Chapters A1.1, A5.2.
(3) Wagner, C.; Hauffe, K. *Z. Elektrochem.* **1939**, *45*, 409.
(4) Tamaru, K. *Adv. Catal.* **1964**, *15*, 65.
(5) Wagner, C. *Adv. Catal.* **1970**, *21*, 323.
(6) Bennett, C. O. *Catal. Rev.* **1976**, *13*, 121.
(7) Kobayashi, M. H.; Kobayashi, H. *Catal. Rev.—Sci. Eng.* **1974**, *10*, 139.
(8) Happel, J.; Walter, E.; Lecouturier, Y. *Ind. Eng. Chem. Fundam.* **1986**, *25*, 704.
(9) Tamaru, K. Dynamic relaxation methods in heterogeneous catalysis. In *Catalysis, Sciences and Technology*; Anderson, J. R., Boudart, M., Eds.; Springer-Verlag: Berlin, 1991; Vol. 9, p 87.
(10) Bennett, C. O. *Adv. Catal.* **1999**, *44*, 329.
(11) Happel, J. In *Isotope Assessment of Heterogeneous Catalysts*; Academic Press: Orlando, FL, 1986.
(12) Biloen, P.; Sachtler, W. M. H. *Adv. Catal.* **1981**, *30*, 203.
(13) Yang, C. H.; Soong, Y.; Biloen, P. *Proceedings of the Eighth International Congress on Catalysis, Berlin*; Ert, G., Ed.; Dechema: Frankfurt-am-Main, 1984; Vol. 2-3.

(14) Biloen, P. *J. Catal*. **1986**, *97*, 330.
(15) Efstathiou, A. M.; Bennett, C. O. *J. Catal*. **1989**, *120*, 137.
(16) Efstathiou, A. M.; Bennett, C. O. *Chem. Eng. Commun*. **1989**, *83*, 129.
(17) Zang, X.; Biloen, P. *J. Catal*. **1986**, *98*, 468.
(18) Stockwell, D. M.; Bennett, C. O. *J. Catal*. **1988**, *110*, 354.
(19) Stockwell, D. M.; Bianchi, D.; Bennett, C. O. *J. Catal*. **1988**, *113*, 13.
(20) Biloen, P.; Helle, J. N.; Van den Berg, A.; Sachtler, W. M. H. *J. Catal*. **1983**, *81*, 450.
(21) Krishna, K. R.; Bell, A. T. *J. Catal*. **1993**, *139*, 104.
(22) Komaya, T.; Bell, A. T. *J. Catal*. **1994**, *146*, 237.
(23) Buess, P.; Caers, R. F. I.; Frennet, A.; Ghenne, E.; Hubert, C.; Kruse, N. U.S. Patent 6,362,239 B1, 2002.
(24) Eigen, M. *Discuss. Faraday Soc*. **1954**, *17*, 194.
(25) Müller, E. W.; Panitz, J. A.; McLane, S. B. *Rev. Sci. Intrum.* **1968**, *39*, 83.
(26) Kruse, N.; Abend, G.; Block, J. H. *J. Chem Phys.* **1989**, *91*, 577.
(27) Margitfalvi, J. F.; Szedacsek, P.; Egedüs, M.; Nagy, F. *Appl. Catal*. **1985**, *15*, 69.
(28) Margitfalvi, J. F.; Szedacsek, P.; Egedüs, M.; Talas, E. Nagy. B. *Proceedings of the Ninth International Congress on Catalysis, Calgary, Canada*; Phillips, M. J., Ternan, M., Eds.; 1988; *Chem. Inst. Can*.: Ottawa, Canada, p 1283.
(29) Frennet, A.; Chitry, V.; Kruse, N. *Appl. Catal. A* **2002**, *229*, 273.
(30) Frennet, A.; Hubert C.; Ghenne, E.; Chitry, V.; Kruse, N. *Proc. 12th Int. Congr. Catal.—Stud. Surf. Sci. Catal., Granada, Spain*; Elsevier: Amsterdam, 2000; Vol. 130, p 3699.
(31) Wilson, J.; de Groot, C. *J. Phys. Chem.* **1995**, *99*, 7860.
(32) Kruse, N.; Abend, G.; Block, J. H. *J. Chem. Phys.* **1988**, *88*, 1307.
(33) Chau, T. D.; Visart de Bocarmé, T.; Kruse, N.; Wang, R. L. C.; Kreuzer, H.-J. *J. Chem. Phys*. **2003**, *119*, 12605.
(34) Frennet, A.; Hubert, C. *J. Mol. Catal. A* **2000**, *163*, 163.
(35) Frennet, A. In *Hydrogen effects in catalysis*; Paal, Z., Menon, P. G., Eds.; Marcel Dekker: New York, 1988.
(36) Beitel, G. A.; Laskov, A.; Osterbeek, H.; Kuipers, E. W. *J. Phys. Chem. B* **1996**, *100*, 12494.
(37) Medvedev, V. K.; Börner, R.; Kruse, N. *Surf. Sci.* **1998**, *401*, L371.
(38) Bridge, M. E.; Comrie, C. M.; Lambert, R. M. *Surf. Sci.* **1977**, *67*, 393.
(39) Liang, D. B.; Abend, G.; Block, J. H. *Surf. Sci*. **1983**, *126*, 392.
(40) Kruse, N.; Gaussmann, A. *J. Catal*. **1993**, *144*, 525.
(41) Block, J. H.; Kruse, N. *React. Kinet. Catal. Lett.* **1987**, *35*, 11.
(42) Frennet, A. In *Elementary reaction steps in heterogeneous catalysis*; Joyner, R. W., van Santen, R. A., Eds.; Kluwer Academic Publisher: Dordrecht, 1993; p 423.
(43) Hubert, C. Ph.D. Thesis, Université Libre de Bruxelles, 1997.
(44) Chitry, V. Ph.D. Thesis, Université Libre de Bruxelles, 2002.
(45) Pearce, R.; Patterson, W. R. In *Catalysis and chemical processes*; Hills, L., Ed.; Wiley: New York, 1981.
(46) Hindermann, J. P.; Hutchings, G. J.; Kienemann, A. *Catal. Rev.—Sci. Eng.* **1993**, *35*, 1.
(47) Friedel, R. A.; Anderson, R. B. *J. Am. Chem. Soc.* **1950**, *72*, 2307.
(48) Pichler, H.; Schulz, H. *Chem.-Ing.-Tech.* **1970**, *42*, 1162.